BIOCHEMISTRY
including biophysical chemistry & molecular biology

Article

pubs.acs.org/biochemistry

Blue Flickers of Hope: Secondary Structure, Dynamics, and Putative Dimerization Interface of the Blue-Light Receptor YtvA from *Bacillus subtilis*

Marcel Jurk,[†,‡] Matthias Dorn,[†,‡] and Peter Schmieder*[,†]

[†]Leibniz-Institut für Molekulare Pharmakologie, Robert-Rössle-Str. 10, 13125 Berlin, Germany

[‡] Institute of Chemistry and Biochemistry, Freie Universität Berlin, Takustr. 3, 14195 Berlin, Germany

Supporting Information

ABSTRACT: *Bacillus subtilis* is capable of responding to various kinds of extracellular, potentially harmful stimuli via a stress response pathway, which involves a signal transduction and integration hub, the stressosome, and finally leads to activation of σ^B. One of the different signals initiating the underlying phosphorylation cascade is blue light. While it is known that the bacterial photoreceptor YtvA is responsible for blue light detection, the intramolecular activation mechanism and the structure of this multidomain protein are unknown. Using solution NMR spectroscopy, we have obtained a near complete backbone assignment of the full-length protein. More importantly, we report relaxation data and data on the solvent accessibility of full-length YtvA in the dark state which are interpreted with respect to secondary structure, the mobility, and the quaternary structure of the protein. Finally, we show that YtvA adopts an elongated domain orientation with LOV−LOV and STAS−STAS interactions on either side.

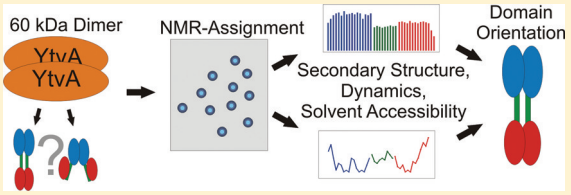

In their natural environment bacteria almost permanently encounter nutrition limitation and physical stress that restricts bacterial growth and force the bacteria to develop appropriate survival strategies. Consequently, various kinds of bacteria have evolved ways to respond to extracellular and potentially life-threatening environmental conditions—sporulation or adaption of the proteome being the most common.[1] *Bacillus subtilis* achieves the stress response via a partner-switching and phosphorylation cascade affecting transcription of up to 150 genes. Salt, energy, and ethanol are the most frequent stress factors.[2] Beside those, blue light has been identified to be one of the extracellular stimuli that provoke or, in the presence of salt stress, enhance the stress response of *B. subitilis in vivo*.[3,4] The photoreceptor−protein YtvA plays an important role in this blue-light-mediated stress response in *Bacillus subtilis* by converting this extracellular stimulus into an intracellular signal.[3,5] Its biological function results from interaction with two of five paralogous proteins from the family of regulators of σ^B (Rsb).[6] These paralogs form a 25 S supramolecular complex of about 1.5 MDa which functions as a signal integration and transduction hub, the so-called stressosome.[7,8]

YtvA comprises 261 residues and consists of an N-terminal LOV (light, oxygen, voltage) and a C-terminal STAS (sulfate transporter/antisigma factor antagonist) domain.[5] The LOV domain acts as the photosensory part of the protein. It harbors FMN as a chromophore which forms a covalent adduct with Cys62 of the protein upon irradiation with blue light.[9] The absorption maximum of the dark, nonsignaling state is 447 nm. Photon absorption and formation of the covalent protein−cofactor adduct cause a hypsochromic shift toward 390 nm. Conversion to the inactive ground state occurs with a half-life of 45 min.[10] The STAS domain contains patches with high sequence identity toward the STAS domains of paralogous Rsb proteins and takes on the role of the effector part of the protein, starting the signal transduction cascade required for σ^B activation. Both domains are connected via a helical linker, called Jα.[11] YtvA is a dimer in solution with a total MW of 60 kDa independent of illumination by blue light.[12]

While the mechanism of light perception by LOV domains is fairly well understood[13,14] it is not clear how the signal received by the LOV domain is transferred to the STAS domain. Until now, no high-resolution structure of any full-length Rsb protein is available, and only models have been proposed.[12,15,16] Studies on isolated LOV domains with the Jα helix attached have suggested that a structural rearrangement in that helix is responsible for signal transduction.[17,18] Other possible mechanisms include rotation of the LOV domains or direct interdomain interactions between the LOV and its output domain.[19,20] Following small-angle X-ray scattering (SAXS) studies in the dark and light-activated state, however, we were able to show that no large structural rearrangements occur as a result of intramolecular signal transduction in the case of YtvA.[12] On the basis of these SAXS data, we presented two possible high-resolution models with completely different conformations that fitted the experimental data equally well. One was termed H-shaped because of the elongated form with

Received: May 20, 2011
Revised: August 2, 2011
Published: August 18, 2011

interactions between both LOV domains on the one and both STAS domains on the other side of the dimer and coiled-coil interactions of Jα in between. The second model was V-shaped with only interactions between the LOV domains. The two STAS domains protruded from either side of the LOV−LOV core. Still, this low-resolution data are not sufficient to understand the activation mechanism on a molecular basis.

Furthermore, it is not clear how the STAS domain functions as an effector domain once the light signal has been received. Interestingly, YtvA lacks the highly conserved threonine residues in the STAS domain that all other paralogs show.[6] Given the fact that the whole σ^B activation process relies on phosphorylation and subsequent partner-switching, questions arise how YtvA may participate in this activation process. Highly conserved within Rsb proteins, on the other hand, is the D_{193}LSG motif of YtvA. Mutations in this area lead to a significant influence on light-mediated stress response or even abolish it completely.[15] It has been discussed that the STAS domain of YtvA might recruit nucleotides for the stressosomal kinase, RsbT, based on its putative NTP-binding capabilities.[21] Recent studies indicate this GTP binding to be only an artifact,[22] which is in line with results obtained in our laboratory [Dorn, 2011, in preparation].

Obviously, high-resolution structural information is necessary to address these questions, which we are trying to obtain using solution-state NMR spectroscopy. Here we present an almost complete assignment of all resonances of the backbone of YtvA in the dark. On the basis of this assignment, we were able to perform a series of experiments that provide information on the secondary structure, the mobility in the two different domains and the linker, and the quaternary structure of this 60 kDa complex. Taken together, these results allow for discrimination between the two proposed orientations by showing that the H-shape model represents the correct overall shape of the dimer in solution.

MATERIALS AND METHODS

Protein Expression and Sample Preparation. The construct of YtvA used in this study comprises amino acids 2 to 261 as in the wild-type protein and an additional Gly at position 1 as left over from the proteolytic cleavage site (TEV). For detailed information on cloning and the resulting construct, see ref 12. Expression of recombinant ^2H,^{13}C,^{15}N-YtvA (DCN-YtvA) or ^2H,^{15}N-YtvA (DN-YtvA) was done using high cell density fermentation (HCDF) utilizing a Dasgip fermentation system *fed batch pro*.[23] T7 Express Rosetta2 cells (New England Biolabs GmbH, Frankfurt a.M., Germany) were used for expression of recombinant protein. Clones for expression were selected according to Sivashanmugam et al.[24] using 70% D_2O-based LB-agar plates supplemented with the appropriate antibotics followed by expression tests. Fermentation was carried out in D_2O (99.98%; Euriso-Top GmbH, Saarbrücken, DE) M9 minimal medium[25] supplemented with 16 g/L ^{13}C-d_{12}-glucose or d_{12}-glucose (Cambridge Isotope Laboratories, Andover, UK), 3.75 g/L $^{15}NH_4Cl$ (Sigma-Aldrich), and additional trace elements.[26] The degree of sample deuteration was estimated to be well above 90% using proton-detected 1D experiments in comparison to experiments acquired for unlabeled protein. Protein sample purification was done as described previously.[12] NMR samples consisted of 500−600 μM specifically labeled YtvA in 20 mM potassium phosphate containing 50 mM NaCl pH 6.5, 0.1% sodium azide, and 5% D_2O. Proton chemical shift was referenced to DSS (2,2-dimethyl-2-silapentane-5-sulfonate) at 0.0 ppm.

NMR Experiments for Chemical Shift Assignments. All NMR spectra were recorded at 27 °C on a Bruker AV 600 MHz spectrometer (Bruker, Karlsruhe, Germany) equipped with a cryo-probehead. The experiments used were all TROSY type[27] and included ^1H−^{15}N-TROSY, HNCACB, HN(CO)-CACB, HNCO, HN(CA)CO, and HNCA(NH) spectra and a ^{15}N-edited NOESY spectrum acquired on DN-YtvA.[28] TOPSPIN (version 2.1, Bruker) was used for data processing, including zero filling and linear prediction. The assignment and general data evaluation were done using the CCPN software package (version 2.1.5).[29]

NMR Chemical Shift Assignment and Data Deposition. A backbone assignment of ^1H_N, ^{15}N, ^{13}CO, $^{13}C_\alpha$, and $^{13}C_\beta$ of 96% of all residues was achieved. The chemical shift data described herein have been deposited in the BioMagResBank[30] under BMRB accession number 17643.

Measurement of Protein Dynamics and Solvent Accessibility. Dynamics of DN-YtvA were assessed using ^{15}N-T1, ^{15}N-T2, and HetNOE experiments[31] recorded as TROSY type. T1 experiments were saturation recovery type and were recorded with delays of 10, 100, 150, 200, 300, 400, 600, 900, 2000, and 5000 ms in an interleaved manner. T2 experiments were also recorded in an interleaved way with delays of 8, 32, 40, 80, 120, 160, 200, and 240 ms. The CCPN software package was used for evaluation of the resulting spectra. Peak intensities at the peak maximum were fitted using CurveFit.[32] TENSOR2[33] was used in a model free approach for calculation of the resulting order parameter S^2.

Inversion recovery experiments with delays of 10, 200, 400, 1200, 1600, and 2000 ms were recorded for DN-YtvA in the presence of 0, 0.5, 1, 2, 5, and 10 mM Magnevist to obtain T1 relaxation times of the individual backbone amide protons dependent on the Gadolinium concentration. Evaluation of the spectra and data was done as described above for T1 experiments. The paramagnetic relaxation enhancement (PRE) effect is a direct result of the Gadolinium-concentration dependent slope of the R1 rates. The slope was calculated using CurveFit.

AUC Experiments for YtvA-STAS. Sedimentation velocity experiments for YtvA-STAS (STAS domain of YtvA; amino acids Gly+148−261) were performed using a Beckman Optima XL-I analytical ultracentrifuge. 800 μL (6 mg/mL) of YtvA-STAS (prepared according to Dorn et al., 2011, in preparation) were dialyzed at 8 °C overnight against 3 L of buffer (20 mM Na-P; 150 NaCl; 2 mM DTT; pH 7.5). Two-sector Epon cells were used at a speed of 50 000 rpm at 12 °C. Data were acquired using the interference optical system (675 nm) with scans taken every 5.5 min. Loading volume was 400 μL of 1 mg/mL (79 μM) and 4 mg/mL (316 μM) YtvA-STAS. Data evaluation was done using the software SEDFIT.[34] Buffer density and viscosity as well as partial specific volume of the protein were calculated using SEDNTERP.[35]

RESULTS

Chemical Shift Assignment. For the extraction of structural and dynamic information from NMR spectra an almost complete assignment is a prerequisite. In case of YtvA, which forms a dimer of 60 kDa, this is not a trivial task. There is, however, a well-established strategy based on protein samples with >95% deuteration of all nonexchangeable protons

used in TROSY-based triple resonance experiments.[27,36,37] Using this strategy, it was possible to obtain spectra with sufficiently narrow lines and dispersion to perform a sequential assignment of the protein backbone. For the actual assignment we mainly relied on the standard triple-resonance experiment pairs HNCACB/HN(CO)CACB and HNCO/HN(CA)CO; additional experiments were used for reasons of clarification. Altogether 96% of all backbone resonances (^1H_N; ^{15}N; C_α; C_β; CO) of the protein were assigned. An $^1H/^{15}N$ TROSY of dark-state YtvA is shown in Figure 1 together with an overview of the assignment.

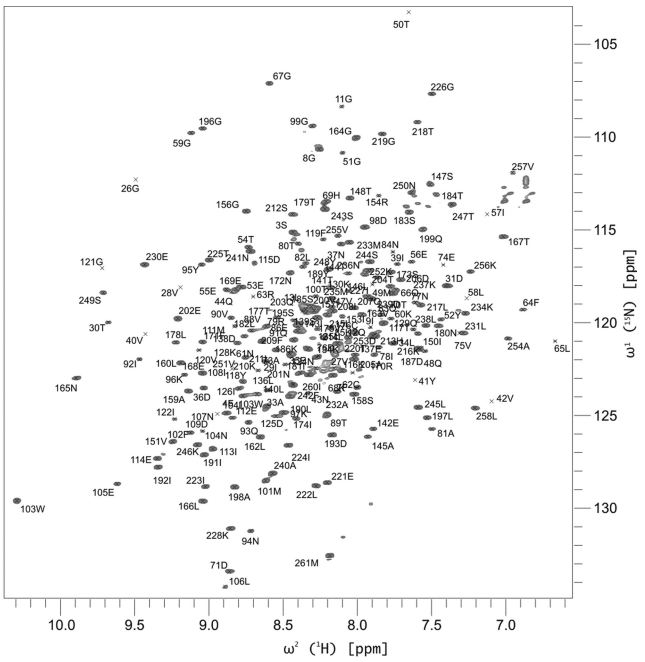

GASFQSFGIP[10] GQLEVIKKAL[20] DHVRVGVVIT[30] DPALEDNPIV[40] YVNQGFVQMT[50]
GYETEEILGK[60] NCRFLQGKHT[70] DPAEVDNIRT[80] ALQNKEPVTV[90] QIQNYKKDGT[100]
MFWNELNIDP[110] MEIEDKTYFV[120] GIQNDITKQK[130] EYEKLLEDSL[140] TEITALSTPI[150]
VPIRNGISAL[160] PLVGNLTEER[170] FNSIVCTLTN[180] ILSTSKDDYL[190] IIDLSGLAQV[200]
NEQTADQIFK[210] LSHLLKLTGT[220] ELIITGIKPE[230] LAMKMNKLDA[240] NFSSLKTYSN[250]
VKDAVKVLPI[260] M

Figure 1. Top: $^1H/^{15}N$-TROSY of 600 μM YtvA(2-261) acquired on a 600 MHz NMR spectrometer (Bruker, Karlsruhe, Germany) labeled with the corresponding sequence positions and amino acid one letter code that results from sequential assignment. Bottom: extent of the ^1H_N; ^{15}N; C_α; C_β; CO assignment of DCN-YtvA from *Bacillus subtilis*. Fully (black) and partially (underlined) assigned residues are highlighted within the amino acid sequence of the protein. A total of 96% of all backbone chemical shifts could be assigned; 97%, 100%, and 98% of LOV(24-127), Jα(128-148), and STAS(149-261), respectively.

In spite of the high level of deuteration, several peaks corresponding to amide protons of the N-terminus and of the Jα linker helix suffered from extensive line broadening. As a consequence, residues 22 to 24 could not be assigned. Relaxation measurements underline this fact, as residues close to these residues show increased ^{15}N-R2 relaxation rates.

Chemical Shift Analysis. Because of the well-known dependency of the chemical shifts of the backbone on the dihedral angles in the protein chain, an assignment can be directly used to determine the secondary structure of a protein.[38] The resulting phi/psi angles from the analysis of the backbone chemical shifts obtained for YtvA using TALOS+[39] are shown in Figure 2 as a comparison to the secondary structure in the proposed model.[15] We used H_N-H_N-NOE information to support the chemical shift analysis.

Given that the available X-ray structure[9] was used as a template for the model of the LOV part of the protein, it is not surprising that there are only minor differences between the typical PAS-fold[40] of the LOV domain and our results. More pronounced differences are present in the Jα helix and the STAS domain. The former appears to be one helical turn longer than predicted extending up to residue 147. Interestingly, part of the N-terminus of YtvA (namely, amino acids 10−21) shows a high propensity to form a helix in solution as indicated by TALOS+ phi/psi angle prediction.

In the STAS domain the β-strands 151−153 and 157−162 appear to be significantly longer, reaching from 149 to 152 and 157 up to 165. NOEs across the strands between amino acids 160 to 165 and 192 to 198 confirm this (see Supporting Information Table S1 for an overview of unambiguous NOEs). In addition, the C-terminal helix can be shown to be shorter, with an elongated stretch of residues at the very end. Another difference we could identify refers to amino acids 241 to 244, which form a helical turn similar to a 3_{10}-helix in the model. TALOS+ prediction clearly points toward an α-Helix. NOEs (see Table S1) underline this assumption.

Independent of the chemical shift analysis, there are also unique NOEs (see Table S1) that indicate spatial closeness of A198 and N165 of ∼4 Å. The homology model and the template (RsbS from *Moorella thermoacetica*; PDB accession code 2VY9)[8] show distances of 8 Å and beyond, respectively, for this part of the STAS domain. The overall structure in this region seems, thus, considerably different.

Relaxation Analysis. To obtain information on the mobility within YtvA, NMR experiments to determine ^{15}N relaxation times were performed,[41] again using TROSY to increase sensitivity and resolution (Table 1). Analysis of spin−spin (T2) and spin−lattice (T1) relaxation experiments for dark-state YtvA results in values characteristic of a multidomain protein with separate domains.[42] Mean R1/R2 (T2/T1) values reflect this with 0.0220 ± 0.007, 0.0138 ± 0.0129, and 0.0135 ± 0.008 for LOV(26-126), Jα(128-149), and STAS(150-261), respectively. The Jα helix exhibits a large variation of values ranging from lower values in the center of this polypeptide linker to higher ones in the direct vicinity of both LOV and STAS domain (see Figure 3, top). Heteronuclear NOEs (HetNOEs) measured for the same sample underline the clear domain differentiation of LOV and STAS. These experiments also reveal a high flexibility of the N- and C-termini of the protein (see Figure 3, middle).

The order parameter (correlation function) S^2, which is calculated from relaxation rates and HetNOEs, is generally acknowledged as a measure for the internal mobility of a specific residue, since relaxation is totally governed by internal motion for $S^2 = 0$ and only by global motion of the protein or domain for $S^2 = 1$.[33] S^2 calculated for YtvA (see Figure 3, bottom) supports the above interpretations with LOV and STAS having different internal mobility with a rigid LOV and a more flexible and "breathing" STAS domain. Average order parameters for LOV and STAS respectively are 0.74 ± 0.10 and 0.60 ± 0.12. The average order parameter of 0.48 ± 0.05 for the Jα linker is even lower than that observed for STAS. The mobility of Jα that is implied by this is not as high as for a fully unstructured and therefore highly mobile peptides as observed for N- or C-terminus.

dx.doi.org/10.1021/bi200782j | *Biochemistry* 2011, 50, 8163−8171

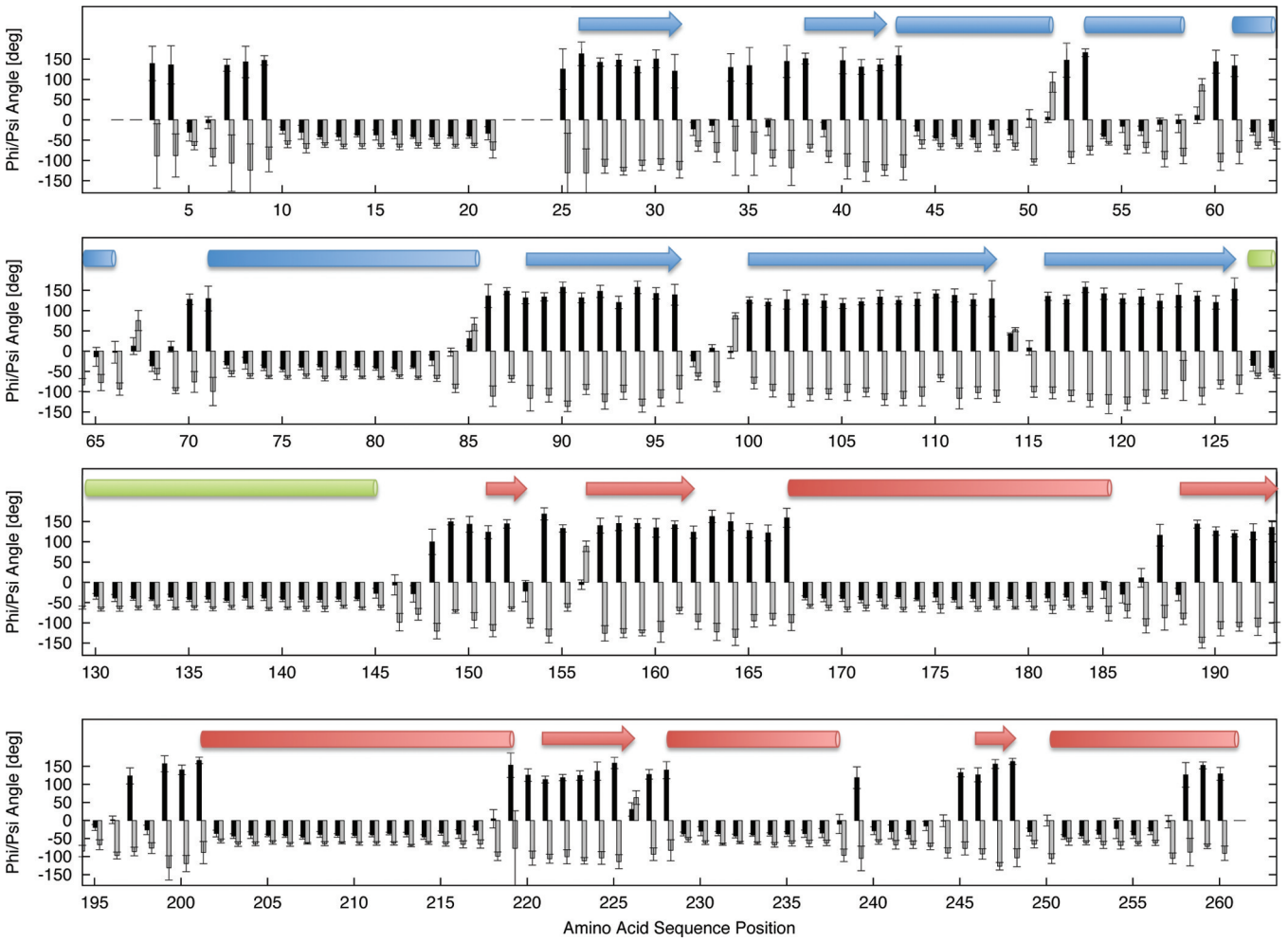

Figure 2. Phi (black) and psi (gray) backbone torsion angles of YtvA based on TALOS+[39] calculations using $^{1}H_{N}$; ^{15}N; C_{α}; C_{β}; CO chemical shift data in comparison to secondary structure calculated from the available model[15] using DSSP[48] (idealized cylinders (α-helix) and arrows (β-strand)). Secondary structure elements belonging to LOV (blue), Jα (green), and STAS (red) are differently colored. Observable differences are discussed in the text. Consecutive patches of similar phi/psi angles indicate presence of secondary structure other than random coil. Typical phi/psi angles are $-55° \pm 10°/-45° \pm 10°$ and $-120° \pm 10°/110° \pm 15°$ for an α-helix or a β-strand, respectively.[49]

Table 1. Overview of the Total Number of Relaxation and SolventPRE Data for the Individual Domains of YtvA[a]

experiment	N-cap(1-23)	LOV(24-127)	Jα(128-148)	STAS(149-261)
relaxation	5	65	8	61
solventPREs	5	77	11	90

[a]The term "relaxation" comprises the number of residues for which a full set of T1, T2, and HetNOE data is available.

Interestingly, a patch between L238 and Y248 within the STAS domain with elevated R1/R2 values and, consequently, higher values for S^2 may be identified. This indicates a lower mobility than for the rest of the STAS domain. The heteronuclear NOE, on the other hand, of the same region shows a local minimum.

Solvent Accessibility. Metal ions that possess an unpaired electron in the outer atomic shell are widely used as contrast agents in medicinal nuclear magnetic imaging. Prominent compounds consisting of a metal ion chelator and a gadolinium[3^{+}] ion (Gd) are Magnevist and Omniscan. We utilized Magnevist following a recently published approach by Madl et al.[43] to examine, first, the extent of solvent accessibility and second to identify putative intramolecular binding interfaces.

The paramagnetic relaxation enhancement (PRE) of Gd depends on r^{-6}, where r is the distance between the Gd and the amide proton observed. Residues on the surface of a protein thus experience a stronger effect than those within the protein. We utilized a standard inversion recovery-type experiment preceding a TROSY pulse sequence to measure proton R1 rates in the presence of different concentrations of Gd. A linear dependency of R1 on the concentration of Gd is observed and can be used to estimate the distance of the amide proton to the solvent accessible surface of the protein. This phenomenon is referred to as solventPRE by Madl et al. to distinguish it from PREs mediated by covalently bound spin-labels as in EPR spectroscopy or in heme binding proteins.[43]

On the basis of the sequence assignment of YtvA, it was possible to calculate a total of 193 solventPREs from a titration with 6 different Gd concentrations (Table 1 and Figure 4). For YtvA the observed values are typically below 0.1 s^{-1} mM $(Gd)^{-1}$ which indicates a well-folded protein. Values higher than this or outliers in general are often observed for residues exhibiting a higher intrinsic mobility and therewith associated exchange with the bulk water surrounding the molecule. Given

dx.doi.org/10.1021/bi200782j | Biochemistry 2011, 50, 8163–8171

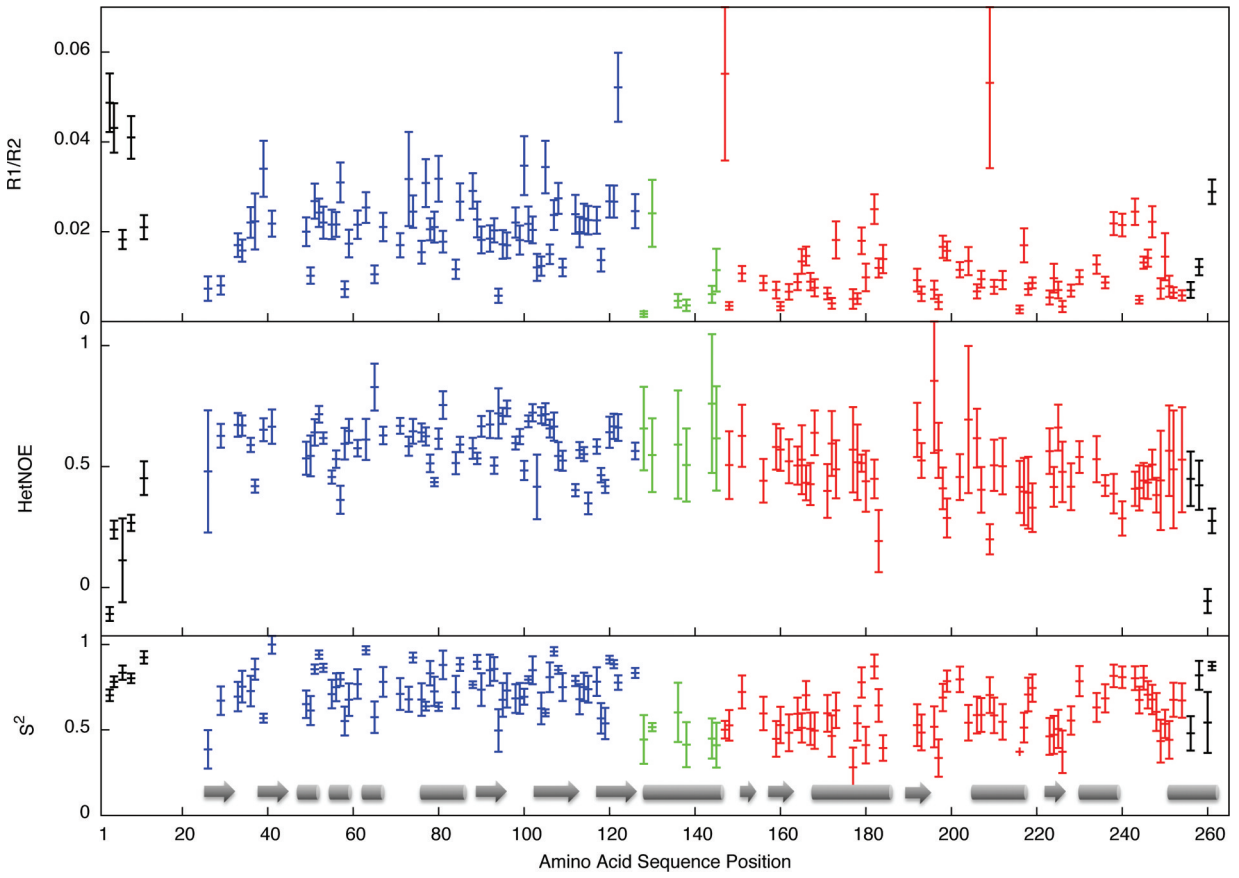

Figure 3. Relaxation data for DN-YtvA in the dark state. Quotient of longitudinal (R1) and transverse (R2) ^{15}N relaxation rates as R1/R2 (top) and (^{1}H)−^{15}N heteronuclear NOEs (middle) are plotted against sequence position. The order parameter S^2 (bottom) was calculated from both R1/R2 and HetNOEs using TENSOR2.[33] The graphical representation highlights the multidomain character of YtvA with different dynamics of LOV (blue), Jα (green), and STAS (red). The flexible N- and C-termini are also displayed (black). Idealized cylinders (α-helix) and arrows (β-strand) indicate the presence of secondary structure as proposed for full-length YtvA.[15] No relaxation analysis was performed for overlapping signals (e.g., amino acids 184 to 192). All underlying data were acquired at 600 MHz.

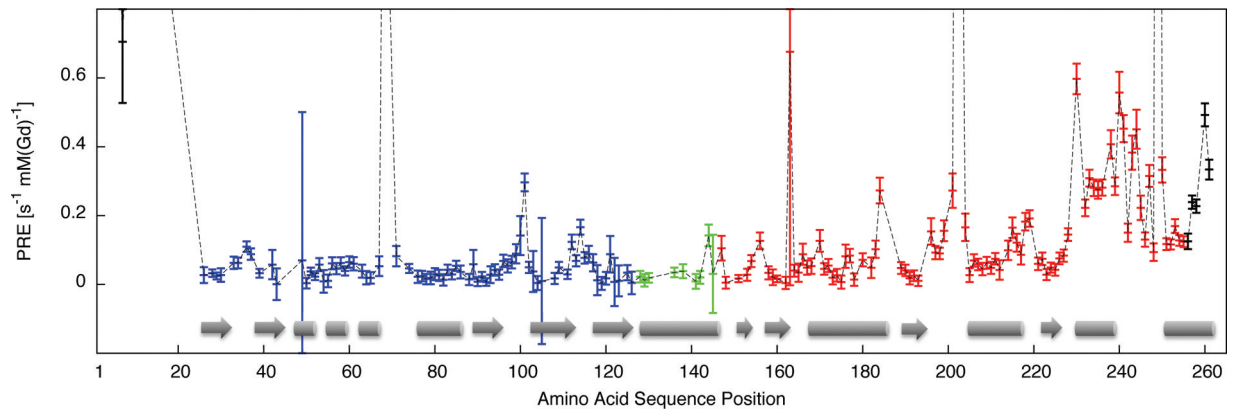

Figure 4. Solvent accessibility of YtvA. Effects of paramagnetic relaxation enhancement (PRE) were assessed by measuring proton longitudinal (R1) relaxation in the presence of different Gadolinium concentrations. The slope in s^{-1} mM $(Gd)^{-1}$ resulting from the linear dependency of R1 on c(Gd) is plotted against sequence position. Outliers well above 0.1 s^{-1} mM $(Gd)^{-1}$ indicate loops or, in general, residues exchanging fast with the surrounding bulk water, which is subjected to intense paramagnetic quenching. LOV (blue), Jα (green), and STAS (red) domain are highlighted. Secondary structure elements as displayed in Figure 2 are indicated as cylinders (α-helix) and arrows (β-strand).

that contrast agents were designed to effectively relax water, this effect is transferred to, in our case, amides that rapidly exchange with water.[43] Residues G99 to M101 (forming the loop between β-strands Gβ and Hβ in the crystal structure[9]) are prominent examples within the otherwise well-structured LOV domain. In general, outliers within the structured regions of LOV and STAS indicate loops.

As already indicated by the relaxation data, this Gd titration also points out that the N-terminus of the protein is highly flexible. The last 30 amino acids of the STAS domain show a similar behavior, also matching the findings of the relaxation

dx.doi.org/10.1021/bi200782j | Biochemistry 2011, 50, 8163–8171

experiments. Whether the comparably high solventPREs are merely caused by water exchange processes could not be elucidated.

Although relaxation data for the Jα linker region point at a high flexibility, the measured solventPREs are not as high as for the STAS C-terminus. This implies that at least parts of the Jα linker are not directly solvent accessible.

The most important finding is that for distinct residues within the β-sheet of the LOV domain very low solventPREs are observed (as low as 0.003 s^{-1} mM $(Gd)^{-1}$ for N104). These residues coincide very well with the core of the LOV−LOV dimer interface as observed in the X-ray structure of truncated YtvA (PDB accession code 2PR5).[9] In contrast, the loop that consists of residues 110 to 119 and connects β-strands H and I shows a rather good solvent accessibility. In solution, the dimer interface between the LOV domains seems therefore restricted to the central part of the β-sheet and the twisted conformation and interactions between end and beginning of β-strands H and I, respectively, only a crystal packing artifact.

As described for the LOV domain, a correspondingly low solvent accessibility is located in the central β-sheet of the STAS domain. Namely, amino acids 191, 192, 159, 160, and 162 form a contiguous patch with solventPREs close to the ones observed for the β-sheet of LOV−LOV dimer interface (e.g., 0.004 s^{-1} mM $(Gd)^{-1}$ for L162). The α-helix at the very C-terminus, which comes to rest directly below this β-sheet in the structural model, on the other hand, shows elevated solvent accessibility for all residues. Moreover, the relaxation data discussed before indicate a high intrinsic mobility of this helix. Thus, it seems unlikely that this helix is shielding the before mentioned β-sheet to provide such low solvent accessibility. As a consequence and in line with the observation for the LOV dimer, formation of a STAS−STAS dimer could explain this finding.

Dimerization of YtvA-STAS. In order to assess the quality of our assumption regarding LOV−LOV and STAS−STAS interactions, we performed analytical ultracentrifugation (AUC) experiments with the sole STAS domain of YtvA (further on called YtvA-STAS; amino acids Gly+148−261). Sedimentation velocity experiments for 1 mg/mL (79 μM) and 4 mg/mL (316 μM) at 50 000 rpm and 12 °C revealed a tendency of YtvA-STAS to dimerize (see Figure S2). At 1 mg/mL a tailing peak in the $c(S)$ distribution plot with a maximum at 1.25 S and a small shoulder at slightly larger S (∼1.8 S) is observable. The molecular mass (MM) can be determined to be 15.6 kDa for the 1.25 S species, while expecting 12.7 kDa. Because of the presence of an associating system, the MM deviation is not unlikely so that this species corresponds to monomeric YtvA-STAS and amounts to 87% of all species present in the solution.[44] About 12.7% relate to the tailing shoulder and less than 0.5% to other species. An increase of the concentration by a factor of 4 results in a $c(S)$ distribution with 57.8% of a 1.27 S and 43.2% of a 1.86 S species. The latter species, which correlates with the shoulder in the $c(S)$ distribution of the 1 mg/mL sample, corresponds to a dimeric YtvA-STAS. A self-association of YtvA-STAS in the low micromolar binding regime (∼350 μM) explains this behavior.

Sedimentation equilibrium experiments for determination of a more exact binding constant yielded no meaningful results. This is most likely due to the intrinsic instability of the YtvA-STAS domain, which is also observed when handling the purified protein. The presence of the LOV domain in full-length YtvA seems to reduce this instability while our relaxation data show that a high flexibility of the STAS domain is still present.

DISCUSSION

The near complete backbone assignment of the 60 kDa multidomain protein YtvA enabled us to use various types of NMR-based methods to characterize the protein in solution. The most important finding directly resulting from our high-resolution NMR-derived data is that we are able to discriminate between the two possible domain orientation models assumed for YtvA and have thus determined the quaternary structure of the protein.

The finding that at least parts of the STAS domain, following secondary and preliminary tertiary structure analysis, show significant differences between our experimental data, and the proposed model explains why some of the results of mutational studies *in vivo* are not fully conclusive.[15] So far the most interesting residues based on this data are D193, S195, and T204, which all result in complete signal transduction loss if exchanged for N, D, or A, respectively. The three amino acids are located directly opposite β-strand 157−161 or above it in case of T204. Any interpretation of this mutations based on a structure/function relation should thus be treated with caution because of the structural differences in this area that result from a change in interactions between amino acids 161−168 and 196−201 and the secondary structure of both.

Our relaxation data consistently suggest a high mobility of the LOV very N-terminus. In addition, we were able to show that a consecutive stretch of about 10 amino acids forms a helix in solution. This is in line with previous assumptions by Buttani et al.[45] Because of signal overlap, we were not able to deduce any information on the dynamics of this helix. Since the first 20 amino acids of YtvA have not been assigned a definite biological function, yet, it is not clear whether or not this part of the protein might be involved in either intra- or intermolecular signal transduction via interactions with the rest of the protein. Recent studies on the photorecovery of different YtvA constructs suggest that the N-terminus has no effect on light activation of the protein.[22] These few amino acids are thus either a redundant relict or play a role in intermolecular signal transduction, which remains to be elucidated.

Relaxation data further indicate that the LOV domain itself is quite rigid while STAS is, in comparison, relatively dynamic. Both are connected via a mobile but structured Jα linker—the latter fact coinciding well with previous findings.[9,19,45] Mobility varies for N- and C-terminus of Jα in comparison to the central part, which suggests that either end of this linker is involved in interactions with LOV and STAS in its N- and C-terminal region, respectively. The central part of the Jα linker shows low R1/R2 rates explaining on the one hand the difficulties to fully assign this region as well as indicating a helical breathing. The same phenomenon is found in the short C-terminal helix of the STAS domain (namely amino acids 251−258). The latter is common to solvent exposed helices in weakly structured regions.[46] Therefore, a concerted motion of the protein in solution seems unlikely. Only residues 238−248 that exhibit a reduced mobility might have a special function during protein activation and signal transduction. It seems unlikely, however, that this region is involved in intramolecular interactions of STAS and LOV domain since elevated solvent accessibility is observed in our Gd experiments.

The Gd experiments also allow us to draw conclusions about the solvent exposure of certain residues of an YtvA dimer and putative interdomain interfaces. In general, the results for the central LOV β-sheet are in agreement with previously published results concerning the oligomeric state of full-length YtvA[12] and the sole LOV domain.[9] Furthermore, this corroborates the assumption to include LOV−LOV contacts in our proposed models as opposed to other experiments based on gel filtration with truncated constructs.[45] Likewise, a low solvent accessibility is found in the STAS β-sheet. The STAS C-terminus, on the other hand, that covers the β-sheet in the homology model shows ubiquitous solvent accessibility and may be classified as flexible based on the relaxation data. Thus, a shielding of the STAS β-sheet by this helix seems unlikely, and the low accessibility could be explained by a putative interface for either LOV−STAS or STAS−STAS interaction. Since no other apparent interface within the LOV domain is evident, a STAS−STAS interaction as occurring in our previously proposed, so-called H-shaped model[12] could explain this experimental finding. In this model dimeric YtvA adopts a dumbbell shape in solution with coiled-coil interactions of Jα and interactions between the β-sheets of the LOV−LOV and STAS−STAS protein part as also proposed by other groups.[8,19] Möglich et al.[9] indisputably proved LOV−LOV interactions for the sole LOV domain. The AUC experiments presented here reveal a self-association of YtvA-STAS, even if significantly lower than for the LOV domains. Since the (sub)nanomolar self-association of the sole LOV domain is also present in the full-length protein (cf. refs 9 and 12) the local concentration of the STAS domain in the full-length protein is significantly increased, resulting in a stronger tendency to dimerize. It is therefore safe to assume that YtvA adopts a dumbbell shape, with LOV−LOV and STAS−STAS interactions on either side. Only a small uncertainty remains as neither solventPREs could be measured for putatively interesting parts of the Jα C-terminus (amino acids 137−148) nor unambiguous NOEs could be identified verifying either binding interface.

In conclusion, we have obtained information on the secondary structure and the mobility within YtvA. On the basis of solvent accessibility and self-association, we show that YtvA is a dimer that has LOV−LOV as well as STAS−STAS contacts and consequently overall corresponds to our proposed H-shape model[12] even though details in the STAS domain in that model are not fully consistent with our data. The independent motion of LOV and STAS, however, emphasizes the question how the signal transduction might occur. Since no major structural rearrangement takes place upon light absorption[12] and it is evident that binding of GTP is not the function of YtvA, the most probable explanation for the effects of light absorption is that there is a structural rearrangement within the YtvA dimer that alters the surface of the protein, in particular of the STAS domain, and thus changes the way the protein is interacting with its partners in the stressosome.

It is obvious that this has to be tested by the determination of the three-dimensional structure of the full-length protein in the dark as well as in the illuminated form. The data presented here in combination with the SAXS data obtained earlier can be used for this. In addition, information from NOE experiments and measurements of residual dipolar coupling will be necessary as well as NOEs involving methyl groups that can be obtained from methyl protonated samples.[47] Work toward this aim is currently in progress in our laboratory.

■ ASSOCIATED CONTENT

Ⓢ Supporting Information

Plots of R1 and R2 rates that underlie R1/R2 depicted in Figure 3, a $c(S)$ distribution for YtvA-STAS obtained using AUC, and a list of H_N-H_N-NOEs. This material is available free of charge via the Internet at http://pubs.acs.org.

■ AUTHOR INFORMATION

Corresponding Author

*Phone +49-30-94793-227. Fax: +49-30-94793-230. E-mail: schmieder@fmp-berlin.de.

Funding

Funding was provided by the Deutsche Forschungsgemeinschaft DFG (SCHM880/8-1).

■ ACKNOWLEDGMENTS

Support from the Leibniz-Institut für Molekulare Pharmakologie is gratefully acknowledged. We thank Drs. Tobias Madl, Anne Diehl, and Wolfgang Gärtner for scientific discussions and Natalja Erdmann and Monika Beerbaum for perfect technical assistance with respect to help with expression of labeled YtvA and implementation of pulse programs, respectively. Magnevist was a generous gift of Dr. Leif Schröder. We are indebted to Wolfgang Bermel (Bruker Biospin) for continuous support in all NMR spectroscopic questions.

■ ABBREVIATIONS

AUC, analytical ultracentrifugation; BMRB, Biological Magnetic Resonance Bank; DN, deuterated ^{15}N-labeled; DCN, deuterated ^{13}C ^{15}N-labeled; Gd, gadolinium; LOV, light, oxygen, voltage; NMR, nuclear magnetic resonance; NOE, nuclear Overhauser effect; HetNOE, heteronuclear NOE; NTP, nucleotide triphosphate; PRE, paramagnetic relaxation enhancement; Rsb, regulators of σ^B; SAXS, small-angle X-ray scattering; STAS, sulfate transporter/antisigma factor antagonist; TEV, tobacco edge virus; TROSY, transverse-relaxation optimized spectroscopy.

■ REFERENCES

(1) Hecker, M., and Völker, U. (2001) General stress response of Bacillus subtilis and other bacteria. *Adv. Microb. Physiol. 44*, 35−91.

(2) Hecker, M., Pané-Farré, J., and Völker, U. (2007) SigB-dependent general stress response in Bacillus subtilis and related gram-positive bacteria. *Annu. Rev. Microbiol. 61*, 215−236.

(3) Avila-Pérez, M., Hellingwerf, K. J., and Kort, R. (2006) Blue light activates the sigmaB-dependent stress response of Bacillus subtilis via YtvA. *J. Bacteriol. 188*, 6411−6414.

(4) Suzuki, N., Takaya, N., Hoshino, T., and Nakamura, A. (2007) Enhancement of a sigma(B)-dependent stress response in Bacillus subtilis by light via YtvA photoreceptor. *J. Gen. Appl. Microbiol. 53*, 81−88.

(5) Losi, A., Polverini, E., Quest, B., and Gärtner, W. (2002) First evidence for phototropin-related blue-light receptors in prokaryotes. *Biophys. J. 82*, 2627−2634.

(6) Akbar, S., Gaidenko, T. A., Kang, C. M., O'Reilly, M., Devine, K. M., and Price, C. W. (2001) New family of regulators in the environmental signaling pathway which activates the general stress transcription factor sigma(B) of Bacillus subtilis. *J. Bacteriol. 183*, 1329−1338.

(7) Chen, C. C., Lewis, R. J., Harris, R., Yudkin, M. D., and Delumeau, O. (2003) A supramolecular complex in the environmental stress signalling pathway of Bacillus subtilis. *Mol. Microbiol. 49*, 1657−1669.

(8) Marles-Wright, J., Grant, T., Delumeau, O., van Duinen, G., Firbank, S. J., Lewis, P. J., Murray, J. W., Newman, J. A., Quin, M. B., Race, P. R., Rohou, A., Tichelaar, W., van Heel, M., and Lewis, R. J. (2008) Molecular architecture of the "stressosome," a signal integration and transduction hub. *Science 322*, 92−96.

(9) Möglich, A., and Moffat, K. (2007) Structural basis for light-dependent signaling in the dimeric LOV domain of the photosensor YtvA. *J. Mol. Biol. 373*, 112−126.

(10) Losi, A., Quest, B., and Gärtner, W. (2003) Listening to the blue: the time-resolved thermodynamics of the bacterial blue-light receptor YtvA and its isolated LOV domain. *Photochem. Photobiol. Sci. 2*, 759−766.

(11) Harper, S. M., Neil, L. C., and Gardner, K. H. (2003) Structural basis of a phototropin light switch. *Science 301*, 1541−1544.

(12) Jurk, M., Dorn, M., Kikhney, A., Svergun, D., Gärtner, W., and Schmieder, P. (2010) The switch that does not flip: the blue-light receptor YtvA from Bacillus subtilis adopts an elongated dimer conformation independent of the activation state as revealed by a combined AUC and SAXS study. *J. Mol. Biol. 403*, 78−87.

(13) Losi, A., and Gärtner, W. (2011) Old Chromophores, New Photoactivation Paradigms, Trendy Applications: Flavins in Blue Light-Sensing Photoreceptors. *Photochem. Photobiol.*, .

(14) Möglich, A., Yang, X., Ayers, R. A., and Moffat, K. (2010) Structure and function of plant photoreceptors. *Annu. Rev. Plant Biol. 61*, 21−47.

(15) Avila-Pérez, M., Vreede, J., Tang, Y., Bende, O., Losi, A., Gärtner, W., and Hellingwerf, K. (2009) In vivo mutational analysis of YtvA from Bacillus subtilis: mechanism of light activation of the general stress response. *J. Biol. Chem. 284*, 24958−24964.

(16) Murray, J. W., Delumeau, O., and Lewis, R. J. (2005) Structure of a nonheme globin in environmental stress signaling. *Proc. Natl. Acad. Sci. U. S. A. 102*, 17320−17325.

(17) Eitoku, T., Nakasone, Y., Zikihara, K., Matsuoka, D., Tokutomi, S., and Terazima, M. (2007) Photochemical intermediates of Arabidopsis phototropin 2 LOV domains associated with conformational changes. *J. Mol. Biol. 371*, 1290−1303.

(18) Harper, S. M., Christie, J. M., and Gardner, K. H. (2004) Disruption of the LOV-Jalpha helix interaction activates phototropin kinase activity. *Biochemistry 43*, 16184−16192.

(19) Möglich, A., Ayers, R. A., and Moffat, K. (2009) Design and signaling mechanism of light-regulated histidine kinases. *J. Mol. Biol. 385*, 1433−1444.

(20) Nash, A. I., McNulty, R., Shillito, M. E., Swartz, T. E., Bogomolni, R. A., Luecke, H., and Gardner, K. H. (2011) Structural basis of photosensitivity in a bacterial light-oxygen-voltage/helix-turn-helix (LOV-HTH) DNA-binding protein. *Proc. Natl. Acad. Sci. U. S. A. 108*, 9449−9454.

(21) Buttani, V., Losi, A., Polverini, E., and Gärtner, W. (2006) Blue news: NTP binding properties of the blue-light sensitive YtvA protein from Bacillus subtilis. *FEBS Lett. 580*, 3818−3822.

(22) Nakasone, Y., and Hellingwerf, K. J. (2011) On the Binding of BODIPY-GTP by the Photosensory Protein YtvA from the Common Soil Bacterium Bacillus subtilis. *Photochem. Photobiol.*, .

(23) Fiedler, S., Knocke, C., Vogt, J., Oschkinat, H., and Diehl, A. (2007) HCDF as a Protein Labeling Methodology, *GEN 27*.

(24) Sivashanmugam, A., Murray, V., Cui, C., Zhang, Y., Wang, J., and Li, Q. (2009) Practical protocols for production of very high yields of recombinant proteins using Escherichia coli. *Protein Sci. 18*, 936−948.

(25) Studier, F. W. (2005) Protein production by auto-induction in high-density shaking cultures. *Protein Expression Purif. 41*, 207−234.

(26) Meyer, O., and Schlegel, H. G. (1983) Biology of aerobic carbon monoxide-oxidizing bacteria. *Annu. Rev. Microbiol. 37*, 277−310.

(27) Pervushin, K., Riek, R., Wider, G., and Wüthrich, K. (1997) Attenuated T2 relaxation by mutual cancellation of dipole-dipole coupling and chemical shift anisotropy indicates an avenue to NMR structures of very large biological macromolecules in solution. *Proc. Natl. Acad. Sci. U. S. A. 94*, 12366−12371.

(28) Zhu, G., and Yao, X. (2008) TROSY-based NMR experiments for NMR studies of large biomolecules. *Prog. Nucl. Magn. Reson. Spectrosc. 52*, 49−68.

(29) Vranken, W. F., Boucher, W., Stevens, T. J., Fogh, R. H., Pajon, A., Llinas, M., Ulrich, E. L., Markley, J. L., Ionides, J., and Laue, E. D. (2005) The CCPN data model for NMR spectroscopy: development of a software pipeline. *Proteins 59*, 687−696.

(30) Ulrich, E. L., Akutsu, H., Doreleijers, J. F., Harano, Y., Ioannidis, Y. E., Lin, J., Livny, M., Mading, S., Maziuk, D., Miller, Z., Nakatani, E., Schulte, C. F., Tolmie, D. E., KentWenger, R., Yao, H., and Markley, J. L. (2008) BioMagResBank. *Nucleic Acids Res. 36*, D402−D408.

(31) Farrow, N. A., Muhandiram, R., Singer, A. U., Pascal, S. M., Kay, C. M., Gish, G., Shoelson, S. E., Pawson, T., Forman-Kay, J. D., and Kay, L. E. (1994) Backbone dynamics of a free and phosphopeptide-complexed Src homology 2 domain studied by 15N NMR relaxation. *Biochemistry 33*, 5984−6003.

(32) Palmer, A. G. (1998) *Program CurveFit: General fitting program for batch use*, Department of Biochemistry and Molecular Biophysics at Columbia University.

(33) Dosset, P., Hus, J. C., Blackledge, M., and Marion, D. (2000) Efficient analysis of macromolecular rotational diffusion from heteronuclear relaxation data. *J. Biomol. NMR 16*, 23−28.

(34) Schuck, P. (2000) Size-distribution analysis of macromolecules by sedimentation velocity ultracentrifugation and lamm equation modeling. *Biophys. J. 78*, 1606−1619.

(35) Hayes, D., Laue, T., Philo, J. (1995) *Program Sednterp: Sedimentation Interpretation Program*, Thousand Oaks, CA.

(36) Gardner, K. H., and Kay, L. E. (1998) The use of 2H, 13C, 15N multidimensional NMR to study the structure and dynamics of proteins. *Annu. Rev. Biophys. Biomol. Struct. 27*, 357−406.

(37) Tugarinov, V., Kanelis, V., and Kay, L. E. (2006) Isotope labeling strategies for the study of high-molecular-weight proteins by solution NMR spectroscopy. *Nature Protoc. 1*, 749−754.

(38) Wishart, D. S., and Sykes, B. D. (1994) Chemical shifts as a tool for structure determination. *Methods Enzymol. 239*, 363−392.

(39) Shen, Y., Delaglio, F., Cornilescu, G., and Bax, A. (2009) TALOS+: a hybrid method for predicting protein backbone torsion angles from NMR chemical shifts. *J. Biomol. NMR 44*, 213−223.

(40) Hefti, M. H., Francoijs, K. J., de Vries, S. C., Dixon, R., and Vervoort, J. (2004) The PAS fold. *Eur. J. Biochem. 271*, 1198−1208.

(41) Palmer, A. G. (2001) Nmr probes of molecular dynamics: overview and comparison with other techniques. *Annu. Rev. Biophys. Biomol. Struct. 30*, 129−155.

(42) Eisenmann, A., Schwarz, S., Prasch, S., Schweimer, K., and Rösch, P. (2005) The E. coli NusA carboxy-terminal domains are structurally similar and show specific RNAP- and lambdaN interaction. *Protein Sci. 14*, 2018−2029.

(43) Madl, T., Bermel, W., and Zangger, K. (2009) Use of relaxation enhancements in a paramagnetic environment for the structure determination of proteins using NMR spectroscopy. *Angew. Chem., Int. Ed. 48*, 8259−8262.

(44) Schuck, P. (2003) On the analysis of protein self-association by sedimentation velocity analytical ultracentrifugation. *Anal. Biochem. 320*, 104−124.

(45) Buttani, V., Losi, A., Eggert, T., Krauss, U., Jaeger, K. E., Cao, Z., and Gärtner, W. (2007) Conformational analysis of the blue-light sensing protein YtvA reveals a competitive interface for LOV-LOV dimerization and interdomain interactions. *Photochem. Photobiol. Sci. 6*, 41−49.

(46) Herrmann, C., Kenneth, R. K., and Markus, R. M. (2006) Can Raman Optical Activity Separate Axial from Local Chirality? A Theoretical Study of Helical Deca-Alanine. *ChemPhysChem 7*, 2189−2196.

(47) Sprangers, R., Velyvis, A., and Kay, L. E. (2007) Solution NMR of supramolecular complexes: providing new insights into function. *Nature Methods 4*, 697−703.

(48) Kabsch, W., and Sander, C. (1983) Dictionary of protein secondary structure: pattern recognition of hydrogen-bonded and geometrical features. *Biopolymers 22*, 2577−2637.

(49) Lovell, S. C., Davis, I. W., Arendall, W. B. III, deBakker, P. I. W., Word, J. M., Prisant, M. G., Richardson, J. S., and Richardson, D. C. (2003) Structure validation by Calpha geometry: phi,psi and Calpha deviation. *Proteins: Struct., Funct., Genet. 50*, 437−450.